Generation and evaluation of multimers of anti C-reactive protein Nb and alkaline phosphatase based on three self-assembly peptides

HONGHE LI[1*], CHENCHEN ZHOU[1*], XIAOMEI ZHANG[1], NING DING[1,2], QIONG WU[1,3], JUNMING LI[4], YANG ZHENG[1] and XUEJUN HU[1,2]

[1]Department of Laboratory Medicine, Medical College, Dalian University, Dalian, Liaoning 116622, P.R. China; [2]Dalian Key Laboratory of Oligosaccharide Recombination and Recombinant Protein Modification, Medical College, Dalian University, Dalian, Liaoning 116622, P.R. China; [3]Research Center, Aim Honesty Biopharmaceutical Co., Ltd., Dalian, Liaoning 116620, P.R. China; [4]Department of Clinical Laboratory, Yantai Yuhuangding Hospital, Yantai, Shandong 264000, P.R. China

Received May 29, 2024; Accepted April 9, 2026

DOI: 10.3892/etm.2026.13279

Abstract. Nanobodies (Nbs) have been extensively utilized in medical diagnosis and therapies due to their advantages, such as ease of genetic manipulation and efficient soluble expression in prokaryotic systems. However, enhancing their binding affinity to antigens to match or even exceed that of polyclonal antibodies for high-sensitivity bioassays remains a challenge. Therefore, in the present study, a novel strategy to enhance the binding affinity of antibodies to antigens was developed by fusing an anti-C-reactive protein Nb (CRPNb) to the N-terminus of self-assembling peptides such as right-handed coiled coil [RHCC; derived from a right-handed coiled-coil peptide of an archaebacterium (*Staphylothermus marinus*)], verotoxin (VTB; the B-subunit of *Escherichia coli* verotoxin) and C4-binding protein (C4bp; derived from human plasma C4-binding protein α-chain). For functional detection, alkaline phosphatase (AP) was further fused to the C-terminus of RHCC, VTB and C4bp, respectively. This approach enabled the formation of CRPNb-RHCC-AP tetramers, CRPNb-VTB-AP pentamers and CRPNb-C4bp-AP heptamers. These were then expressed as soluble cytoplasmic proteins in the *E. coli* strain BL21 (DE3) and purified by imidazole elution. The protein expression was assessed by western blotting. Additionally, the stability of the multimeric constructs was evaluated using a direct ELISA, whilst their sensitivity was assessed using a competitive ELISA. The CRPNb-VTB-AP pentamers and CRPNb-RHCC-AP tetramers demonstrated antigen-specific recognition and enhanced affinity compared with the CRP-AP monomer based on a direct ELISA. Furthermore, they exhibited good thermal stability based on a direct ELISA. At 80˚C, CRPNb-VTB-AP, CRPNb-AP and CRPNb-RHCC-AP retained ~85, 75 and 60% activity, while CRPNb-H only retained ~40%. After incubation at 80˚C for 55 min, the two multimers still maintained ~40% activity. The results suggested them to be suitable for storage and transportation at ambient temperatures. In conclusion, a novel nanobody-fusion protein platform was established in the present study. The fusion proteins functioned as high-affinity binders for target antigens and heat-stable signal tracers for immunoassay detection and quantitative analysis, providing a novel type of thermostable immunoreagent.

Correspondence to: Professor Xuejun Hu, Dalian Key Laboratory of Oligosaccharide Recombination and Recombinant Protein Modification, Medical College, Dalian University, 10 Xuefu Street, Dalian, Liaoning 116622, P.R. China
E-mail: huxuejun@dlu.edu.cn

Dr Xiaomei Zhang, Department of Laboratory Medicine, Medical College, Dalian University, 10 Xuefu Street, Dalian, Liaoning 116622, P.R. China
E-mail: zhangxiaomei@dlu.edu.cn

*Contributed equally

Key words: nanobody, multimerization, C reactive protein nanobody, self-assembling peptides

Introduction

Nanobodies (Nbs) originate from the variable region fragments of heavy chain-only antibodies [variable domain of heavy chain-only antibody (VHH)] originally found in camelid mammals (1). They represent the smallest class of natural antibody fragments, possessing high degrees of antigen-binding specificity and affinity (1,2). Nbs typically have a molecular weight of ~15 kDa and can recognize hidden antigen epitopes that are challenging for conventional antibodies to detect. This capability has driven their increasingly popular application in diagnosing and treating various diseases, including breast cancer, brain tumours, lung diseases and infectious diseases (3-6). However, due to their small molecular size, Nbs have a short serum half-life and exhibit 10^2-10^3 times lower binding affinity to antigens compared with polyclonal antibodies, limiting their effectiveness in highly sensitive bioassays (7-9).

Multimerization is an attractive approach for enhancing the performance of Nbs, which is garnering interest in this field (10). A number of methods (2,5,11,12) for creating multimers have been proposed, with the most common being the

formation of multimers through the use of self-assembling peptides (12,13). At present, the most commonly used Nb multimeric peptides include right-handed coiled coil (RHCC), verotoxin (VTB), C4-binding protein (C4bp) and cartilage oligomeric matrix protein (COMP) (14,15). Wang *et al* (12) previously produced single-domain antibodies derived from camel antibody variable domains fused with three different polypeptides (RHCC, COMP and C4bp), which in turn generated tetramers, pentamers and heptamers. These multimeric constructs were successfully expressed in prokaryotic expression systems (BL21) (12), with all recombinant polymers maintaining their antigen-specific recognition. Another previous study demonstrated that C4bp can enhance the multimerization of Nbs. This multimerization can further improve Nb resistance to hydrolysis, stability, affinity and sensitivity (16).

Fusing alkaline phosphatase (AP) or HRP to Nbs can streamline the detection process because the time is reduced as only one incubation step is required, eliminating intermediate washing steps, shortening the overall detection time and enhancing detection sensitivity (15,17). To date, various Nbs fused with AP, HRP or other tag proteins have been tested for food safety analysis and human health diagnosis (17), such as Nb-AP, Nb with streptavidin binding peptide, Nb-HRP, Nb-nanosized luciferase and super folder green fluorescent protein (GFP)-Nb (1,18-28). Notably, AP is widely used in fluorescence immunoassays. This enzyme catalyzes the dephosphorylation of fluorogenic substrates, yielding strong and detectable fluorescent signals that can be quantitatively measured (29,30).

C-reactive protein (CRP) is a key biomarker for inflammation, the accurate quantification of which is crucial during infections and healing processes (31). The present study provides a comprehensive account of the construction, expression, purification and evaluation of Nbs specific to CRP (CRPNb)-VTB-AP, CRPNb-C4bp-AP and CRPNb-RHCC-AP multimers. These constructs are based on self-assembling peptide domains, namely RHCC, VTB and C4bp, using CRPNb as the VHH derived from a non-immune llama VHH library and AP as the detection tag (an example with pentamers is shown in Fig. S1). The aim of the present study was to enhance the performance of Nb multimers for improved functionality.

Materials and methods

Reagents. The cDNA sequence encoding the Nb specific to human CRP (31) and the cDNA sequence for ALP of *Escherichia coli*, which exhibited a 35-fold increase in specific activity after substituting the serine for the completely invariant Asp101 using site-directed mutagenesis, were previously prepared (32). Sangon Biotech Co., Ltd., provided the *E. coli* strain BL21 (DE3) used in the present study. The PCL expression plasmids were synthesized based on the sequence of pIG6 (33,34), with the Amp resistance gene replaced by the kanamycin resistance gene in the new vector. Our laboratory (Dalian Key Laboratory of Oligosaccharide Recombination and Recombinant Protein Modification, Medical College, Dalian University, Dalian, Liaoning, China) maintained the PCL-PelB-anti VHHs plasmid.

The cDNA sequences for anti-CRPNb-VTB-AP-histidine (H), CRPNb-C4bp-H, CRPNb-H and CRPNb-RHCC-H were obtained from Sangon Biotech Co., Ltd., and inserted into the PCL-PelB-antiGFP VHHs vector using the restriction enzymes *Bam*HI and *Xho*I. The cDNA sequences for VTB (35), RHCC self-assembled peptide (36) and C4bp (17) were synthesized based on the published peptides sequences (Table SI). Restriction enzymes, DNA ligation kit reagents and various enzymes (such as LA Taq and T4 Polynucleotide Kinase) were purchased from Takara Biotechnology Co., Ltd., whilst isopropyl thio-β-D-galactoside (IPTG), kanamycin and additional reagents (such as NaCl, NaH_2PO_4 and KH_2PO_4) were sourced from Sangon Biotech Co., Ltd.

Construction of plasmids. The PCL-PelB-CRPNb-VTB-AP-H and PCL-PelB-CRPNb-H vectors were subsequently digested with the restriction enzymes *Bam*HI and *Eco*RI, yielding the fragments PCL-PelB-CRPNb, AP-H and PCL-PelB-CRPNb-H, respectively. T4 DNA Ligase was used to ligate the CRPNb and AP-H fragments, forming CRPNb-AP-H. Finally, the CRPNb-AP-H fragment was inserted into the PCL-PelB-anti-GFP VHHs vector using the restriction enzymes *Bam*HI and *Xho*I to form PCL-PelB-CRPNb-AP-H. The recombinant plasmid was then transformed into *E. coli* strain BL21 (DE3) and positive clones were selected on Luria-Bertani (LB) plates containing 50 μg/ml kanamycin from Sangon Biotech Co., Ltd. Monoclonal clones were picked for digestion analysis, before the positive clones were sent to Sangon Biotech Co., Ltd., for DNA sequencing identification using Sanger sequencing.

Expression and purification. The protocols for the expression and purification of CRPNb-H, CRPNb-AP-H, CRPNb-RHCC-AP-H, CRPNb-VTB-AP-H and CRPNb-C4bp-AP-H were largely identical. BL21 (DE3) cells harboring the PCL-PelB vectors containing CRPNb-H, PCL-PelB-CRPNb-RHCC-AP-H, PCL-PelB-CRPNb-VTB-AP-H,PCL-PelB-CRPNb-C4bp-AP-H and PCL-PelB-CRPNb-AP-H were grown overnight in LB medium (Sangon Biotech Co., Ltd.), supplemented with the appropriate antibiotics such as kanamycin (50 μg/ml), at 37˚C with shaking at 220 rpm. The following day, the culture was inoculated at a ratio of 1:100 into a medium containing 500 ml LB liquid medium and 50 μg/ml kanamycin and incubated at 37˚C with shaking until the cell optical density (OD) detected using the multifunctional microplate detector SpectraMax® Plus 384 (Molecular Devices, LLC) at 600 nm reached ~0.6. IPTG was then added to a final concentration of 0.2 mM, before 200 ml culture was harvested after 6 h of induction at 25˚C. The pellet was resuspended in PBS (0.02 M KH_2PO_4 and 0.02 M Na_2HPO_4; pH=7.4) and then lysed by sonication on ice for 15 min of 3-sec pulses with 2-sec intervals at 36 W. The lysate was collected and centrifuged at 12,000 x g at 4˚C for 10 min. The supernatant was recovered as the 'soluble' fraction. After washing once with ice-cold PBS, the pellets were re-suspended in 80 μl ice-cold PBS and designated as the 'insoluble' fraction. An equal volume of 40 mM imidazole was added to the supernatant to a final concentration of 20 mM before filter sterilization. Tween-20 was then added into the supernatant to a final concentration of 3%. The HisTrap

Excel (Sigma-Aldrich; Merck KGaA) and injection tubing were washed with ultrapure water filtered through a 0.45-μm membrane, and then equilibrated with binding buffer (0.02 M PBS, 0.5 M NaCl; pH 7.4) at a flow rate of 1 ml/min for a total volume of 20 ml. The supernatant was loaded onto the column, followed by washing with 20 mM imidazole at a flow rate of 2 ml/min for a volume of 20 ml. An elution buffer with different concentrations of imidazole (20, 40 and 80 mM) was then added to the column to elute the target proteins. Protein concentrations were measured using the BCA assay with BSA (Thermo Fisher Scientific, Inc.) as standard.

Western blotting. The samples corresponding to purified CRPNb-H, CRPNb-AP-H, CRPNb-RHCC-AP-H, CRPNb-VTB-AP-H and CRPNb-C4bp-AP-H were mixed with 20 μl 5X loading buffer separately and boiled for 10 min. After cooling to room temperature, 8-μl samples were separated on a 15% polyacrylamide gel and transferred onto a PVDF membrane. For the control (CRPNb-VTB-AP-H), 20 μl (240 μg/ml) was loaded. Following blocking of non-specific binding sites with 5% skim milk in TBS with Tween-20 (TBST) buffer (20 mM Tris-HCl pH 8.0, 150 mM NaCl, 0.05% Tween-20) for 2 h at room temperature, the PVDF membrane was further incubated with anti-His antibody (MA1-21315; Thermo Fisher Scientific, Inc.) diluted 1:4,000 in TBST buffer for 1 h at room temperature. The membrane was then washed eight times (5 min each) in TBST buffer prior to incubation with the secondary antibody conjugated to horseradish peroxidase (31430; Thermo Fisher Scientific, Inc.) diluted 1:4,000 in TBST buffer for 40 min at room temperature. An enhanced chemiluminescence kit (Shanghai Epizyme Biopharmaceutical Technology Co., Ltd.; Ipsen Pharma) and a system with Image Lab™ image capture software (version 5.2.1; Bio-Rad Laboratories, Inc.) were used for signal detection. Semi-quantitative gray analysis was performed with ImageJ software (v1.8.0; National Institutes of Health). These data are derived from at least three replicate experiments.

Nb activity. A direct ELISA was used to assess the activity of the CRPNb-RHCC-AP tetramers, CRPNb-C4bp-AP heptamers and CRPNb-VTB-AP pentamers. CRP antigen at 5 μg/ml was added to 96-well microplates and the plates were incubated at 4˚C for 24 h. Following this, serial dilutions of the multimers (100 μl/well) were added and the plates were incubated for 2 h at 37˚C. After washing the plates with PBS containing 0.05% Tween 20 (PBST), the microplates were incubated with a polyclonal anti-His-tag antibody (100 μl/well; diluted 1:3,000 in PBS; MA1-21315; Thermo Fisher Scientific, Inc.) at 37˚C for 1 h. Subsequently, the plates were washed again with PBST, before an HRP-conjugated goat anti-mouse secondary antibody (diluted 1:5,000 in PBST; 31430; Thermo Fisher Scientific, Inc.) was added and plates were incubated at 37˚C for 1 h.

After rinsing the plates with PBST, 100 μl 3,3',5,5'-tetramethylbenzidine substrate solution was added to each well and plates were incubated at 37˚C for 10 min. The chromogenic reaction was immediately stopped by adding 50 μl 2 M H_2SO_4 to each well. The OD of the final solution was measured at 450 nm using a multifunctional microplate reader (SpectraMax®Plus 384; Molecular Devices, LLC).

AP activity. The AP activity of the CRPNb-RHCC-AP tetramers, CRPNb-VTB-AP pentamers and CRPNb-C4bp-AP heptamers was assessed using a calorimetric assay with p-nitrophenyl phosphate (pNPP; Dalian Meilun Biology Technology Co., Ltd.). Briefly, various concentrations (0, 0.312, 0.625, 1.25, 2.5, 5.0 and 10 μM) of the CRPNb-RHCC-AP tetramers, CRPNb-VTB-AP pentamers and CRPNb-C4bp-AP heptamers were added to 96-well microplates at 100 μl/well. Subsequently, 50 μl/well of a 2.7-mM pNPP solution (pH 9.8), containing 1 M diethanolamine and 0.5 mM $MgCl_2$, was added. After incubation at 37˚C for 10 min, the chromogenic reaction was terminated by adding 3 M NaOH to each well at 50 μl/well. The OD of the solution was then measured at 405 nm using a multifunctional microplate reader.

Thermal stability. The thermal stability of the CRPNb-RHCC-AP tetramers, CRPNb-VTB-AP pentamers and CRPNb-C4bp-AP heptamers was evaluated using two different heat treatment methods. Initially, eight aliquots of the CRPNb-RHCC-AP tetramers, CRPNb-VTB-AP pentamers and CRPNb-C4bp-AP heptamers were subjected to heating at 25, 30, 40, 50, 60, 70, 80 and 90˚C for 5 min each. In total, 10 aliquots of the CRPNb-RHCC-AP tetramers, CRPNb-VTB-AP pentamers and CRPNb-C4bp-AP heptamers were heated at 80˚C for 0, 5, 15, 25, 35, 45, 55 and 65 min. Subsequently, the activity of the Nb was assessed as aforementioned. The remaining Nb activity was calculated using the following equation: Remaining Nb activity (%)=[(OD450 of heat-treated multimers)/(OD450 of untreated multimers)] x100%.

Effect of pH and PBS on the Nb activity of multimers. A direct ELISA was conducted to evaluate the impact of pH and PBS concentration on the Nb activity. A 5 μg/ml solution of CRP antigen was added to a 96-well microplate (442404; Thermo Fisher Scientific, Inc.), which was then incubated at 4˚C for 24 h. Following this, serial concentrations of multimers (100 μl/well) were added, with varying pH (4, 5, 6, 7, 7.4, 8, 9 and 10) and PBS concentrations (2X, 1X, 0.5X and 0.25X). The procedure outlined in the Nb activity subsection was followed for the remaining steps. The remaining Nb activity was calculated using the following equation: Remaining Nb activity (%)=[(OD450 of treated multimers)/(OD450 of untreated multimers)] x100%.

Detection efficiency of multimers. A competitive ELISA was conducted according to previously established methods (15). A checkerboard titration was utilized to determine the optimal concentration of the coating antigen and multimers. CRP (0, 0.25, 0.50, 1.0, 2.0, 5.0 and 10.0 μg/ml) and multimers (0.25, 0.5, 1.0, 2.0 and 5.0 μg/ml) were diluted at different concentrations for ELISAs to determine the optimal concentration of the coating antigen and multimers. Subsequently, the reaction conditions were optimized, including the antigen and antibody concentration (5, 2.5 or 1.25 μg/ml CRP; 3, 1.5 or 0.75 μg/ml pentamers), blocking solution (3% BSA, 1.5% BSA, 5% skim milk powder or 2.5% skim milk powder), competitive reaction duration (30, 60 or 120 min), pH value (6.0, 7.0, 7.4, 8.0 or 9.0) and PBS concentration (2X, 1X or 0.5X).

After overnight coating of the plates (442404; Thermo Fisher Scientific, Inc.) at 4˚C with 100 μl CRP coating antigen (2.5 μg/ml), the plate was blocked with 5% skimmed milk at

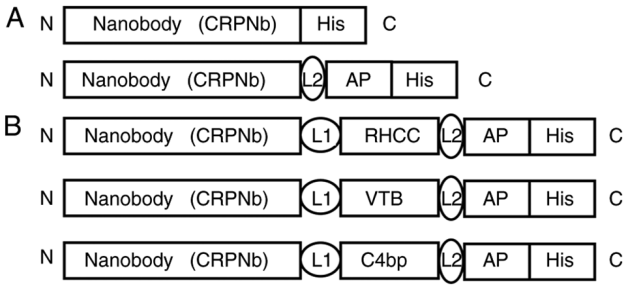

Figure 1. (A) Primary structure of the CRPNb and CRPNb-AP nanobodies. (B) Primary structure of the recombinant multimers (top, CRPNb-RHCC-AP; middle, CRPNb-VTB-AP; bottom, CRPNb-C4bp-AP). CRPNb, C-reactive protein nanobody; AP, alkaline phosphatase; RHCC, right-handed coiled coil; VTB, verotoxin; C4bp, C4-binding protein; N, N-terminus; C, C-terminus; L, linker; L1, APKADNKGGGGS; L2, APKADNKEFGGGGS; His, polyhistidine purification tag.

37˚C for 2 h. The plates were washed five times with PBST. Subsequently, 50 μl CRP and 50 μl fusion proteins, namely CRPNb-AP, CRPNb-C4bp-AP, CRPNb-VTB-AP and CRPNb-RHCC-AP, were added to each well. After incubation at room temperature for 1 h, the plates were rinsed three times with PBST, and 100 μl pNPP substrate (5 μg/ml in ethanol) was added and plates were incubated at 37˚C for 15 min. The reaction was stopped by adding 50 μl NaOH, and the absorbance was measured at 405 nm using a SpectraMax®Plus 384 microplate reader (Molecular Devices, LLC).

Results and Discussion

Construction and expression of multimers. The cDNA sequences for anti-CRPNb-VTB-AP-H, CRPNb-C4bp-H, CRPNb-H and CRPNb-RHCC-H were obtained from Sangon Biotech Co., Ltd., and inserted into the PCL-PelB-antiGFP VHHs vector using the restriction enzymes *Bam*HI and *Xho*I. The recombinant plasmids PCL-CRPNb-RHCC-AP, PCL-CRPNb-VTB-AP and PCL-CRPNb-C4bp-AP were successfully introduced into *E. coli* BL21 (DE3) for the expression of tetramers, pentamers and heptamers of CRPNb-RHCC-AP, CRPNb-VTB-AP and CRPNb-C4bp-AP, respectively. The expression and purification of these multimers were then analyzed using western blotting. In the present study, CRPNb, which was derived from llama and specifically targets CRP, was used (24). The linear schematic of the proposed CRPNb and CRPNb-AP peptides is shown in Fig. 1A. Using self-assembling peptides RHCC, VTB or C4bp, CRPNb and AP were then fused to obtain recombinant constructs CRPNb-RHCC-AP, CRPNb-VTB-AP and CRPNb-C4bp-AP, respectively. The linear peptide schematics of these recombinant multimers are shown in Fig. 1B. In addition, linker 1 (APKADNKGGGGS) and linker 2 (APKADNKEFGGGGS) are derived from protein A, and can separate the different domains. Based on their amino acid composition, the calculated molecular weights of CRPNb, CRPNb-AP, CRPNb-RHCC-AP, CRPNb-VTB-AP and CRPNb-C4bp-AP are 12.85, 65.29, 72.38, 74.47 and 73.15 kDa, respectively.

Western blotting was performed using the mouse anti-His tag antibody and a precipitated ECL substrate solution. The predicted thick bands, corresponding to ~12, 65, 72, 74 and 73 kDa, matching the molecular weights of CRPNb, CRPNb-AP, CRPNb-RHCC-AP tetramers, CRPNb-VTB-AP pentamers and CRPNb-C4bp-AP heptamers, respectively, could be observed (Fig. 2A). Based on a previous study, it can be inferred that β-mercaptoethanol and heating lead to the complete degradation of the CRPNb-RHCC-AP multimers, CRPNb-VTB-AP pentamers and CRPNb-C4bp-AP heptamers into monomers (37). Although native PAGE was not performed in the present study, previous studies have confirmed that these recombinant constructs can efficiently self-assemble into specific oligomers: Tetramers mediated by RHCC, pentamers mediated by VTB and heptamers mediated by C4bp (15-18,35,37-41). Correspondingly, the genes fused with RHCC, VTB and C4bp can successfully express the tetrameric, pentameric and heptameric target proteins, respectively.

The recombinant proteins (CRPNb-AP, CRPNb-VTB-AP and CRPNb-C4bp-AP) were found to be expressed in both soluble and insoluble forms (Fig. 2B). CRPNb-RHCC-AP was found to be expressed in the soluble form (Fig. 2B). The soluble fraction was sonicated and the supernatant was subsequently purified. The purification process involved elution with imidazole using a HisTrap Excel column, followed by BCA protein quantification. In the present study, the relative expression levels of the multimers were determined using purified CRPNb-VTB-AP as a control (Fig. 2B). The relative protein expression levels for the soluble fraction normalized to the control were as follows: 2.1 for the CRPNb-RHCC-AP tetramers, 3.0 for the CRPNb-VTB-AP pentamers, 0.5 for the CRPNb-C4bp-AP heptamers and 2.7 for CRPNb-AP. The proportions of soluble to insoluble components for CRPNb-VTB-AP, CRPNb-C4bp-AP and CRPNb-AP were found to be 3.06, 0.63 and 2.16, respectively. The proportion of soluble to insoluble components could not be calculated for CRPNb-RHCC-AP because the level of the insoluble components was too low.

In the present study, CRPNb-VTB-AP exhibited the highest level of soluble components among the CRPNb-RHCC-AP tetramers, CRPNb-VTB-AP pentamers and CRPNb-C4bp-AP heptamers.

The protein levels of CRPNb-RHCC-AP tetramers and CRPNb-C4bp-AP heptamers aligned with previous findings, which reported successful expression and proper folding of tetrameric EG2 [an anti-epidermal growth factor receptor single-domain antibody (sdAb)]-RHCC and heptameric EG2-C4bp in prokaryotic expression systems such as BL21 and *E. coli* TG1 (12,38). Zhang *et al* (39) previously developed a multimerization strategy and used size-exclusion chromatography to characterize the formation of pentamers.

Characterization of CRPNb-RHCC-AP tetramers, CRPNb-C4bp-AP heptamers and CRPNb-VTB-AP pentamers. The antibody activities of the CRPNb-RHCC-AP tetramers, CRPNb-VTB-AP pentamers and CRPNb-C4bp-AP heptamers were next examined and compared with those of CRPNb-H. Fig. 3 shows that CRPNb-H exhibited a markedly higher OD450 signal compared with CRPNb-VTB-AP, CRPNb-RHCC-AP tetramers and CRPNb-C4bp-AP heptamers, suggesting a superior antigen-binding ability. Additionally, the OD450 for CRPNb-VTB-AP was slightly

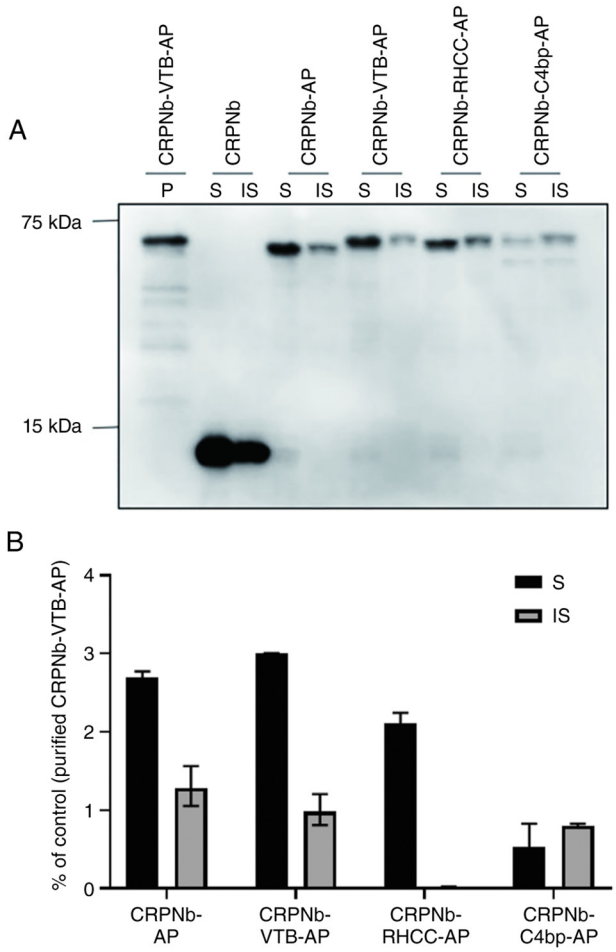

Figure 2. (A) Western blot analysis was conducted to examine the fusion proteins of CRPNb, CRPNb-AP, CRPNb-RHCC-AP, CRPNb-VTB-AP and CRPNb-C4bp-AP using purified CRPNb-VTB-AP as a molecular weight standard for reference. (B) Relative expression levels of CRPNb-AP, CRPNb-RHCC-AP, CRPNb-VTB-AP and CRPNb-C4bp-AP. Proteins were quantified using purified CRPNb-VTB-AP [lane P in (A)] as a control. The concentration of the control protein CRPNb-VTB-AP was 240 μg/ml, as determined by a BCA assay. Image Lab software was used for the intensity analysis. CRPNb, C-reactive protein nanobody; AP, alkaline phosphatase; RHCC, right-handed coiled coil; VTB, verotoxin; C4bp, C4-binding protein; S, soluble; IS, insoluble; P, positive control.

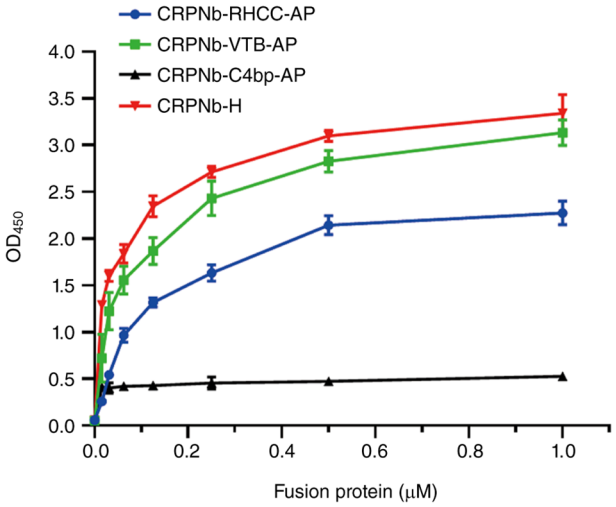

Figure 3. Direct ELISA used to measure the activity of the monomeric and multimeric Nbs. Error bars indicate the standard deviation of three replicates of the experiment. OD, optical density; CRPNb, C-reactive protein nanobody; AP, alkaline phosphatase; RHCC, right-handed coiled coil; VTB, verotoxin; C4bp, C4-binding protein; H, histidine.

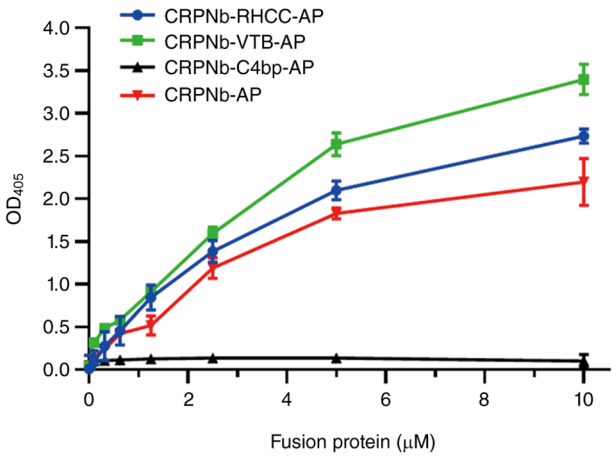

Figure 4. AP activity of the monomeric and multimerized antibodies as measured using a calorimetric assay with p-nitrophenyl phosphate. Error bars indicate the standard deviation of three replicates of the experiment. OD, optical density; CRPNb, C-reactive protein nanobody; AP, alkaline phosphatase; RHCC, right-handed coiled coil; VTB, verotoxin; C4bp, C4-binding protein.

higher compared with that of CRPNb-RHCC-AP, suggesting that CRPNb-VTB-AP had a stronger antigen-binding capacity compared with CRPNb-RHCC-AP. By contrast, CRPNb-C4bp-AP exhibited no antigen-binding capacity, which is inconsistent with previous studies (15-17). The enzymatic activities of the CRPNb-RHCC-AP tetramers, CRPNb-VTB-AP pentamers and CRPNb-C4bp-AP heptamers were next examined and compared with those of CRPNb-AP. Fig. 4 shows that CRPNb-RHCC-AP tetramers and CRPNb-VTB-AP pentamers exhibited higher enzyme activity compared with CRPNb-AP. The CRPNb-C4bp-AP heptamers exhibited no AP activity, contradicting previous studies (15,17). Due to experimental constraints, the control group in Fig. 3 was CRPNb-H. However CRPNb-AP should have been employed as the control to align with Fig. 4, which would have made the experiment more scientifically sound and reasonable. Therefore, the results, such as Fig. 3 showing that CRPNb-H exhibited a markedly higher OD450 signal compared with CRPNb-VTB-AP, CRPNb-RHCC-AP tetramers and CRPNb-C4bp-AP heptamers, have certain limitations. If the control group were replaced with CRPNb-AP, the results might have been different.

As shown in Fig. 4, the AP activity of CRPNb-RHCC-AP tetramers and CRPNb-VTB-AP pentamers was increased compared with that of CRPNb-AP. This indicated that AP fusion with the multimeric domain did not impair AP activity in the CRPNb-RHCC-AP tetramers and CRPNb-VTB-AP pentamers. Compared with findings from previous studies (29,36), the present study revealed that CRPNb-C4bp-AP heptamers exhibited both a lack of antigen-binding capacity and no AP activity. There are a number of possible reasons for these observations. The position of CRPNb and AP at either the N- or C-terminus of

C4bp may have impacted their activity (18). In addition, the spatial structure of the CRPNb-C4bp-AP fusion protein may have affected the key amino acid sites responsible for CRP recognition in the heptamers. Furthermore, the flexible linker may not have adequately separated the functional regions of CRPNb and AP, potentially impacting the key amino acid sites involved in CRP recognition due to interference from the fusion expression with AP. In summary, the pentameric CRPNb-VTB-AP demonstrated superior AP activity and CRP binding ability compared with the other multimers tested.

Stability of multimers

Thermal stability. Two distinct heat treatment methods were used for the thermal stability testing of CRPNb-RHCC-AP tetramers, CRPNb-VTB-AP pentamers and CRPNb-C4bp-AP heptamers. As shown in Fig. 5A, the Nb activity of the CRPNb-RHCC-AP tetramers, CRPNb-VTB-AP pentamers and CRPNb-C4bp-AP heptamers decreased with increasing temperature. As the temperature increased, ~85% of the activity of the CRPNb-VTB-AP pentamers, ~75% of the activity of CRPNb-AP and ~60% of the activity of the CRPNb-RHCC-AP tetramers was maintained even at 80˚C, whilst the activity of CRPNb-H dropped to ~40%. Based on these results, the impact of incubation time at 80˚C on the binding activity between the antigen and antibody was further examined. Fig. 5B shows that after 55 min of incubation at 80˚C, ~40% of the activity was retained for the CRPNb-RHCC-AP tetramers and CRPNb-VTB-AP pentamers. This suggested that the multimeric Nbs were thermostable, suggesting that they may be suitable for long-term storage at room temperature.

Effect of pH and PBS on Nb activity. To evaluate the influence of pH on the analysis performance, the effect of pH on the assay was evaluated over a range of pH 4 to 10 using the optimized assay buffer by direct ELISA. The binding signal of the antibody at pH 7.4 was defined as 100%, and the binding activity at other pH conditions was expressed as the percentage relative to this value, denoted as % binding activity at room temperature (RT). As shown in Fig. 6, the % RT binding of the CRPNb-RHCC-AP tetramers and CRPNb-VTB-AP pentamers was increased from 69 to 105% and 70.5 to 102% as the pH of the assay buffer increased from pH 4 to 8, before decreasing from pH 9 onwards. By contrast, the binding of CRPNb-H, CRPNb-C4bp-AP and CRPNb-AP was increased from 50, 53 and 62 to 100% as the pH of the assay buffer increased from 4 to 7.4, before decreasing from pH 7.4 onwards, suggesting that pH affected Nb binding activity. Therefore, pH 7.4 was chosen as the optimal pH for the assay buffer. Similarly, different concentrations of PBS were next optimized (Fig. 7). The OD450 absorbance of the CRPNb-RHCC-AP tetramers, CRPNb-VTB-AP pentamers and CRPNb-AP was slightly increased as the concentration of PBS decreased from 2X to 1X PBS, then decreased from 1X to 0.25X PBS. Therefore, 1X PBS was selected as the optimal PBS concentration.

Comparative analysis of the detection performance of monomers and multimers. To assess the detection performance of the monomers and multimers, a competitive ELISA was used to evaluate the inhibition curves of the CRPNb-RHCC-AP tetramers, CRPNb-VTB-AP pentamers and CRPNb-C4bp-AP heptamers. The optimal concentrations of the coating antigen and antibody were determined using checkerboard titration (Fig. S2). The optimal antigen concentration was 2 μg/ml and the optimal antibody concentration was 1 μg/ml. At these concentrations, the absorbance value approached 1. Fig. S3 presents an experimental study on conditional optimization using CRPN-VTB-AP pentamers as a case study. Appropriate experimental conditions were selected for subsequent competitive ELISAs. As shown in Fig. 8, the CRPNb-VTB-AP pentamers exhibited the highest sensitivity, with an IC_{50} of 11.86 ng/ml, compared with CRPNb-AP and CRPNb-RHCC-AP, which had IC_{50} values of 45.47 and 23.86 ng/ml, respectively. Compared with the CRPNb-AP monomer, these values were 4X lower for CRPNb-VTB-AP and 2X lower for CRPNb-RHCC-AP. This suggested that

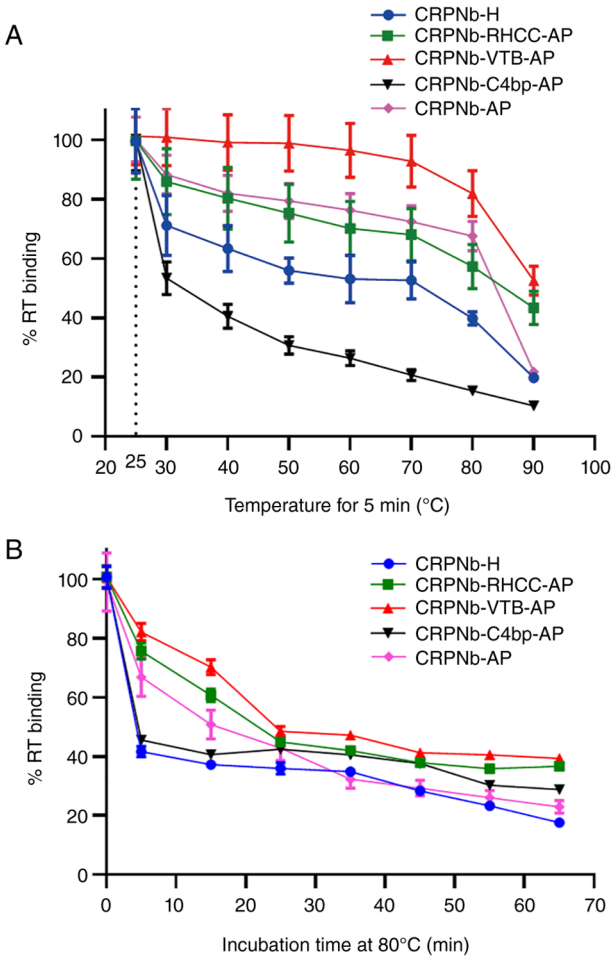

Figure 5. (A) Each of the five fusion proteins was incubated for 5 min at various temperatures, before the temperature stability of different Nbs was compared. The binding value obtained after treatment at room temperature (25˚C) was used as the 100% binding control. % RT binding refers to the binding value relative to that at room temperature (25˚C). (B) Each of the five fusion proteins was incubated for the indicated durations at 80˚C, before the temperature stability of different Nbs was compared. The binding value at 0 min after treatment at 80˚C was used as the 100% binding control. % RT binding refers to the binding value relative to that at 0 min after treatment at 80˚C. Error bars indicate the standard deviation of three replicates of the experiment. Nb, nanobodies; CRPNb, C-reactive protein nanobody; AP, alkaline phosphatase; RHCC, right-handed coiled coil; VTB, verotoxin; C4bp, C4-binding protein; H, histidine; RT, room temperature.

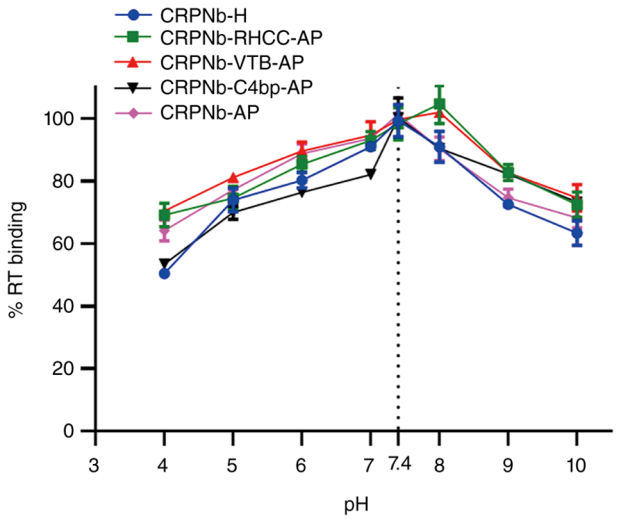

Figure 6. Comparison of nanobody-antigen activity of fusion proteins under different pH conditions. The binding signal of the antibody at pH 7.4 (physiological pH) was set as 100%, and % RT binding refers to the ratio of the binding signal under other pH conditions to that at pH 7.4. Error bars indicate the standard deviation of three replicates of the experiment. CRPNb, C-reactive protein nanobody; AP, alkaline phosphatase; RHCC, right-handed coiled coil; VTB, verotoxin; C4bp, C4-binding protein; H, histidine; RT, room temperature.

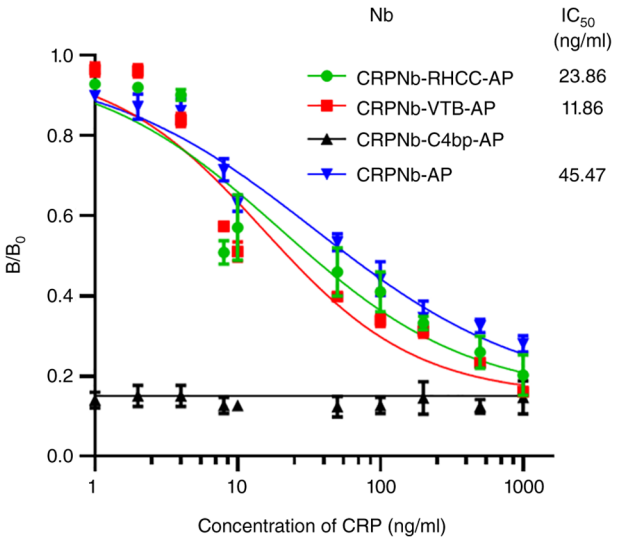

Figure 8. Comparative analysis of the sensitivity of monomer and fusion proteins by competitive ELISA. Error bars indicate the standard deviation of three replicates of the experiment. The y-axis represents B/B_0, which is the ratio of the bound signal intensity at a given CRP concentration (B) to the maximum bound signal intensity in the absence of competing free CRP (B_0, normalized to 1.0). Nb, nanobody; CRP, C-reactive protein; CRPNb, CRP nanobody; AP, alkaline phosphatase; RHCC, right-handed coiled coil; VTB, verotoxin; C4bp, C4-binding protein.

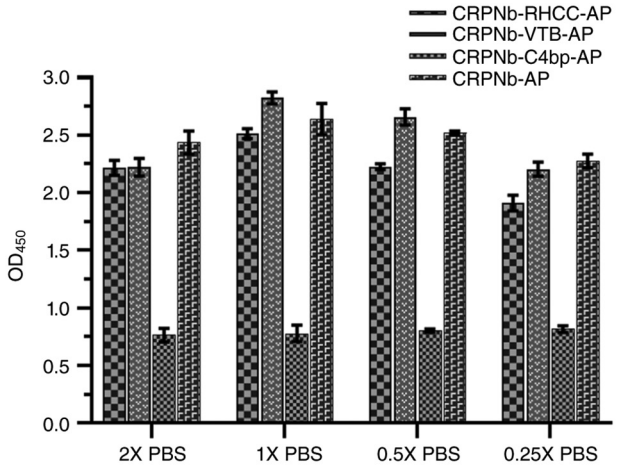

Figure 7. Comparison of Nb-antigen activity of fusion proteins under different PBS concentrations. Error bars indicate the standard deviation of three replicates of the experiment. CRPNb, C-reactive protein nanobody; AP, alkaline phosphatase; RHCC, right-handed coiled coil; VTB, verotoxin; C4bp, C4-binding protein; OD, optical density.

multimerization strategies could effectively enhance the affinity of Nbs to antigens. The increased affinity of Nbs is essential for improving the sensitivity of immunodetection. Nb multimers from previous studies have demonstrated improved antigen affinity and detection sensitivity compared with monomers (40,41), which is consistent with the results observed in the present study.

In the present study, recombinant CRPNb-RHCC-AP tetramers, CRPNb-VTB-AP pentamers and CRPNb-C4bp-AP heptamers were successfully constructed using the three self-associating peptides RHCC, VTB and C4bp. Within the cytoplasm, these peptides are likely to adopt the right conformation and are purified as soluble proteins, thus avoiding laborious denaturation and refolding procedures, making the process both cost-effective and environmentally friendly (10,33).

In future studies, non-denaturing PAGE should be used to verify the multimer products. Additionally, the CRPNb-VTB-AP pentamers and CRPNb-RHCC tetramers demonstrated antigen-specific recognition and enhanced affinity compared with the CRP-AP monomer. Furthermore, all three multimers exhibited thermal stability, making them suitable for storage and transportation at ambient temperatures. This platform enables the fusion of Nbs with various detection tags, allowing for the generation of multimers with different combinations of Nbs and different tags. By selecting compatible Nbs and self-assembling peptides, Nb activity, enzyme activity, binding affinity and detection performance can be optimized. This approach may lead to the development of bio-functional immune reagents that serve as both high-affinity binders and sensitive tracers.

Although previous studies have studied tetramers, pentamers and heptamers based on RHCC, VTB and C4bp using other Nbs such as EG2-sdAb (13) with AP or other tags, to the best of our knowledge, the present study is the first to form tetramers, pentamers and heptamers using CRPNb and AP based on the three self-assembled peptides and to assess the activity of CRP and AP. The present study aimed to establish a platform for identifying the most effective multimers with superior antigen-binding capabilities and increased AP activity. This will facilitate the development of sensitive and reliable detection methods for CRP.

Acknowledgements

Not applicable.

Funding

Funding for the present study was provided by the National Natural Science Foundation of China (grant nos. 32070936, 32270985 and 32201050), the Dalian Science and Technology Innovation Fund of China (grant no. 2022JJ13S N07 0), the Yantai Science and Technology Innovation Development Plan (Policy Guidance) Project (grant no. 2023YD025), the Educational Department of Liaoning Province (grant no. JYTQN2023103) and the Department of Science & Technology of Liaoning Province (grant no. 2025-MSLH-026).

Availability of data and materials

The data generated in the present study may be requested from the corresponding author.

Authors' contributions

XZ, XH, HL and CZ were involved in the design of the study. XZ and XH were involved in the conception of the study. ND, QW, JL and YZ were involved in all the biological experiments and in data analysis. HL, CZ and XZ were involved in the writing of the manuscript. XZ and XH supervised all experiments and confirmed the authenticity of all the raw data. All authors have read and approved the final version of the manuscript.

Ethics approval and consent to participate

Not applicable.

Patient consent for publication

Not applicable.

Competing interests

The authors declare that they have no competing interests.

References

1. Liu X, Xu Y, Wan DB, Xiong YH, He ZY, Wang XX, Gee SJ, Ryu D and Hammock BD: Development of a nanobody-alkaline phosphatase fusion protein and its application in a highly sensitive direct competitive fluorescence enzyme immunoassay for detection of ochratoxin A in cereal. Anal Chem 87: 1387-1394, 2015.
2. Els Conrath K, Lauwereys M, Wyns L and Muyldermans S: Camel single-domain antibodies as modular building units in bispecific and bivalent antibody constructs. J Biol Chem 276: 7346-7350, 2001.
3. Huo J, Li Z, Wan D, Li D, Qi M, Barnych B, Vasylieva N, Zhang J and Hammock BD: Development of a highly sensitive direct competitive fluorescence enzyme immunoassay based on a nanobody-alkaline phosphatase fusion protein for detection of 3-phenoxybenzoic acid in urine. J Agric Food Chem 66: 11284-11290, 2018.
4. Jovčevska I and Muyldermans S: The therapeutic potential of nanobodies. BioDrugs 34: 11-26, 2020.
5. Chanier T and Chames P: Nanobody engineering: Toward next generation immunotherapies and immunoimaging of cancer. Antibodies (Basel) 8: 13, 2019.
6. Naidoo DB and Chuturgoon AA: The potential of nanobodies for COVID-19 diagnostics and therapeutics. Mol Diagn Ther 27: 193-226, 2023.
7. Sun Z, Wang X, Chen Q, Yun Y, Tang Z and Liu X: Nanobody-alkaline phosphatase fusion protein-based enzyme-linked immunosorbent assay for one-step detection of ochratoxin A in rice. Sensors (Basel) 18: 4044, 2018.
8. Nuñez-Prado N, Compte M, Harwood S, Álvarez-Méndez A, Lykkemark S, Sanz L and Álvarez-Vallina L: The coming of age of engineered multivalent antibodies. Drug Discov Today 20: 588-594, 2015.
9. Deyev SM and Lebedenko EN: Multivalency: The hallmark of antibodies used for optimization of tumor targeting by design. Bioessays 30: 904-918, 2008.
10. Arbabi-Ghahroudi M: Camelid single-domain antibodies: Historical perspective and future outlook. Front Immunol 8: 1589, 2017.
11. Bathula NV, Bommadevara H and Hayes JM: Nanobodies: The future of antibody-based immune therapeutics. Cancer Biother Radiopharm 36: 109-122, 2021.
12. Wang L, Liu X, Zhu X, Wang L, Wang W, Liu C, Cui H, Sun M and Gao B: Generation of single-domain antibody multimers with three different self-associating peptides. Protein Eng Des Sel 26: 417-423, 2013.
13. Asano R, Koyama N, Hagiwara Y, Masakari Y, Orimo R, Arai K, Ogata H, Furumoto S, Umetsu M and Kumagai I: Anti-EGFR scFv tetramer (tetrabody) with a stable monodisperse structure, strong anticancer effect, and a long in vivo half-life. FEBS Open Bio 6: 594-602, 2016.
14. Li C, Feng H, Xia X, Wang L, Gao B, Zhang Y and Lan X: (99m) Tc-labeled tetramer and pentamer of single-domain antibody for targeting epidermal growth factor receptor in xenografted tumors. J Labelled Comp Radiopharm 59: 305-312, 2016.
15. Bao K, Liu X, Xu Q, Su B, Liu Z, Cao H and Chen Q: Nanobody multimerization strategy to enhance the sensitivity of competitive ELISA for detection of ochratoxin A in coffee samples. Food Control 127: 108167, 2021.
16. Li Z, Wang Y, Vasylieva N, Wan D, Yin Z, Dong J and Hammock BD: An ultrasensitive bioluminescent enzyme immunoassay based on nanobody/nanoluciferase heptamer fusion for the detection of tetrabromobisphenol A in sediment. Anal Chem 92: 10083-10090, 2020.
17. Su B, Bei Z, Pei H, Xie X, Sun Z, Chen Q, Cao H and Liu X: Generation of a nanobody-alkaline phosphatase heptamer fusion for ratiometric fluorescence immunodetection of trace alpha fetoprotein in serum. Int J Biol Macromol 201: 507-515, 2022.
18. Su B, Xu H, Xie G, Chen Q, Sun Z, Cao H and Liu X: Generation of a nanobody-alkaline phosphatase fusion and its application in an enzyme cascade-amplified immunoassay for colorimetric detection of alpha fetoprotein in human serum. Spectrochim Acta A Mol Biomol Spectrosc 262: 120088, 2021.
19. Wang J, Majkova Z, Bever CRS, Yang J, Gee SJ, Li J, Xu T and Hammock BD: One-step immunoassay for tetrabromobisphenol a using a camelid single domain antibody-alkaline phosphatase fusion protein. Anal Chem 87: 4741-4748, 2015.
20. Sheng Y, Wang K, Lu Q, Ji P, Liu B, Zhu J, Liu Q, Sun Y, Zhang J, Zhou EM and Zhao Q: Nanobody-horseradish peroxidase fusion protein as an ultrasensitive probe to detect antibodies against Newcastle disease virus in the immunoassay. J Nanobiotechnology 17: 35, 2019.
21. Mu Y, Jia C, Zheng X, Zhu H, Zhang X, Xu H, Liu B, Zhao Q and Zhou EM: Correction to: A nanobody-horseradish peroxidase fusion protein-based competitive ELISA for rapid detection of antibodies against porcine circovirus type 2. J Nanobiotechnology 19: 66, 2021.
22. Sun Z, Lv J, Liu X, Tang Z, Wang X, Xu Y and Hammock BD: Development of a nanobody-AviTag fusion protein and its application in a streptavidin-biotin-amplified enzyme-linked immunosorbent assay for ochratoxin A in cereal. Anal Chem 90: 10628-10634, 2018.
23. Chen Q, Sun D, Pei H, Su B, Bao K, Cao H, Zhang C, Hammock BD and Liu X: Development of a nanobody tagged with streptavidin-binding peptide and its application in a Luminex fluoroimmunoassay for alpha fetal protein in serum. RSC Adv 10: 23767-23774, 2020.
24. Chen Q, Wang Y, Mao F, Su B, Bao K, Zhang Z, Xie G and Liu X: Development of a horseradish peroxidase-nanobody fusion protein for visual detection of ochratoxin A by dot immunoassay. RSC Adv 10: 33700-33705, 2020.
25. Su B, Zhang Z, Sun Z, Tang Z, Xie X, Chen Q, Cao H, Yu X, Xu Y, Liu X and Hammock BD: Fluonanobody-based nanosensor via fluorescence resonance energy transfer for ultrasensitive detection of ochratoxin A. J Hazard Mater 422: 126838, 2022.

26. Yu S, Li Z, Li J, Zhao S, Wu S, Liu H, Bi X, Li D, Dong J, Duan S and Hammock BD: Generation of dual functional nanobody-nanoluciferase fusion and its potential in bioluminescence enzyme immunoassay for trace glypican-3 in serum. Sens Actuators B Chem 336: 129717, 2021.
27. Aydın EB, Aydın M and Sezgintürk MK: Highly selective and sensitive sandwich immunosensor platform modified with MUA-capped GNPs for detection of spike Receptor Binding Domain protein: A precious marker of COVID 19 infection. Sens Actuators B Chem 345: 130355, 2021.
28. Wang X, Wang Y, Wang Y, Chen Q and Liu X: Nanobody-alkaline phosphatase fusion-mediated phosphate-triggered fluorescence immunoassay for ochratoxin a detection. Spectrochim Acta A Mol Biomol Spectrosc 226: 117617, 2020.
29. Xiao T, Sun J, Zhao J, Wang S, Liu G and Yang X: FRET effect between fluorescent polydopamine nanoparticles and MnO_2 nanosheets and its application for sensitive sensing of alkaline phosphatase. ACS Appl Mater Interfaces 10: 6560-6569, 2018.
30. Zhang Z, Su B, Xu H, He Z, Zhou Y, Chen Q, Sun Z, Cao H and Liu X: Enzyme cascade-amplified immunoassay based on the nanobody-alkaline phosphatase fusion and MnO_2 nanosheets for the detection of ochratoxin A in coffee. RSC Adv 11: 21760-21766, 2021.
31. Oloketuyi S, Bernedo R, Christmann A, Borkowska J, Cazzaniga G, Schuchmann HW, Niedziółka-Jönsson J, Szot-Karpińska K, Kolmar H and de Marco A: Native llama nanobody library panning performed by phage and yeast display provides binders suitable for C-reactive protein detection. Biosensors (Basel) 11: 496, 2021.
32. Mandecki W, Shallcross MA, Sowadski J and Tomazic-Allen S: Mutagenesis of conserved residues within the active site of *Escherichia coli* alkaline phosphatase yields enzymes with increased kcat. Protein Eng 4: 801-804, 1991.
33. Chao S, Liu Y, Ding N, Lin Y, Wang Q, Tan J, Li W, Zheng Y, Hu X and Li J: Highly expressed soluble recombinant anti-GFP VHHs in *Escherichia coli* via optimized signal peptides, strains, and inducers. Front Mol Biosci 9: 848829, 2022.
34. Zhu J, Ruan Y, Fu X, Zhang L, Ge G, Wall JG, Zou T, Zheng Y, Ding N and Hu X: An engineered pathway for production of terminally sialylated N-glycoproteins in the periplasm of *Escherichia coli*. Front Bioeng Biotechnol 8: 313, 2020.
35. Zhang J and Mackenzie CR: Multivalent display of single-domain antibodies. Methods Mol Biol 911: 445-456, 2012.
36. Mayr J, Lupas A, Kellermann J, Eckerskorn C, Baumeister W and Peters J: A hyperthermostable protease of the subtilisin family bound to the surface layer of the archaeon *Staphylothermus marinus*. Curr Biol 6: 739-749, 1996.
37. Kielkopf CL, Bauer W and Urbatsch IL: Sodium dodecyl sulfate-polyacrylamide gel electrophoresis of proteins. Cold Spring Harb Protoc 2021: 494-504, 2021.
38. Stone E, Hirama T, Chen W, Soltyk AL, Brunton J, MacKenzie CR and Zhang J: A novel pentamer versus pentamer approach to generating neutralizers of verotoxin 1. Mol Immunol 44: 2487-2491, 2007.
39. Zhang J, Li Q, Nguyen TD, Tremblay TL, Stone E, To R, Kelly J and Roger MacKenzie C: A pentavalent single-domain antibody approach to tumor antigen discovery and the development of novel proteomics reagents. J Mol Biol 341: 161-169, 2004.
40. Wang F, Li ZF, Wan DB, Vasylieva N, Shen YD, Xu ZL, Yang JY, Gettemans J, Wang H, Hammock BD and Sun YM: Enhanced non-toxic immunodetection of Alternaria mycotoxin tenuazonic acid based on ferritin-displayed anti-idiotypic nanobody-nanoluciferase multimers. J Agric Food Chem 69: 4911-4917, 2021.
41. Fan K, Jiang B, Guan Z, He J, Yang D, Xie N, Xie C and Yan X: Fenobody: A ferritin-displayed nanobody with high apparent affinity and half-life extension. Anal Chem 90: 5671-5677, 2018.